Manufacturing of Ultrasound- & MRI-Compatible Aortic Valves Using 3D Printing for Analysis & Simulation

Shu Wang[1], Harminder Gill[1], Weifeng Wan[2], Helen Tricker[1], Joao Filipe Fernandes[1], Yohan Noh[1], Sergio Uribe[3], Jesus Urbina[3], Julio Sotelo[3], Ronak Rajani[1], Pablo Lamata[1], Kawal Rhode[1]

[1]School of Biomedical Engineering & Imaging Sciences, King's College London, London, UK
[2]Department of Materials, Imperial College London, London, UK
[3]Biomedical Imaging Centre, Pontificia Universidad Catolica de Chile, Santiago, Chile

Abstract. Valve-related heart disease affects 27 million patients worldwide and is associated with inflammation, fibrosis and calcification which progressively lead to organ structure change. Aortic stenosis is the most common valve pathology with controversies regarding its optimal management, such as the timing of valve replacement. Therefore, there is emerging demand for analysis and simulation of valves to help researchers and companies to test novel approaches. This paper describes how to build ultrasound- and MRI-compatible aortic valves compliant phantoms with a two-part mold technique using 3D printing. The choice of the molding material, PVA, was based on its material properties and experimentally tested dissolving time. Different diseased valves were then manufactured with ecoflex silicone, a commonly used tissue-mimicking material. The valves were mounted with an external support and tested in physiological flow conditions. Flow images were obtained with both ultrasound and MRI, showing physiologically plausible anatomy and function of the valves. The simplicity of the manufacturing process and low cost of materials should enable an easy adoption of proposed methodology. Future research will focus on the extension of the method to cover a larger anatomical area (e.g. aortic arch) and the use of this phantom to validate the non-invasive assessment of blood pressure differences.

Keywords: Aortic Stenosis, Valve Fabrication, 3D Printing, US-MRI Compatible.

1 Background & Introduction

Aortic stenosis (AS) is the most common valve-related disease, associated with inflammation, fibrosis and calcification, which can lead to progressive organ structure change [1]. AS can result from differing underlying pathologies and the macroscopic appearance is typically classified into one of the following categories: calcified valve, rheumatic valve and bicuspid valve. The prevalence of aortic stenosis increases with age, and if left untreated high mortality is observed [2]. Moreover, left ventricular outflow tract obstruction increases the workload of the left ventricle ultimately leading to heart failure [3]. Treatment of the valve, by means of surgical or minimally invasive methods, is required as no pharmacological methods demonstrate efficacy at preventing progression. However, current diagnostic methods are inadequate regarding optimal management, such as the timing of valve replacement. In-vitro studies of valve disease and pre-procedural interventional planning can benefit from advances in 3D printing [4]. Due to the need of ultrasound- and MRI- compatibility, compliance, flexibility and durability when connected to a hemodynamic pump, the valve material needs to be chosen carefully while the valve shape should be realistic. Silicone is an optimal material because it is a room temperature-vulcanized material with stiffness similar to soft tissue [5]. However, the structure of the aortic valve is complicated and direct silicone printing technology is not available in the current market.

Despite the current technical limitation of rapid prototyping and 3D printing in the literature [6], it offers a significant tool for making and validating pathological valves, as well as an important education tool for trainees involved in the treatment of valvular disease. Given the difficulties of making a durable and compliant aortic valve model, several patient-specific tissue-mimicking phantoms were previously printed directly using TangoPlus and VeroBlackPlus, which can achieve a layer thickness of 30 microns. However, replication of these methods requires high printing cost even though these two materials are reported to be much stiffer than ecoflex silicone [7]. Motivated by practicing the surgical procedure, a detailed soft organ phantom was created by a technique of 3D wax printing and polymer molding [8]. The outer molds are printed with VeroClear and the inner molds are printed with wax. But the wax molding material needs to be dissolved in ethanol at 70 ℃, which makes it more complicated and potentially unachievable in most labs.

Here, we present a low-cost and simple two-part mold-based technology of manufacturing a realistic aortic valve and with the use of PVA, the internal mold can be easily dissolved in water at room temperature. Besides a normal silicone valve, some typical pathological valves were also fabricated for comparison and the imaging compatibility was validated using both ultrasound and MRI. 3D-printable PVA was chosen as the molding material for its easy printability, fast water-soluble property, as well as the good performance under great external forces. The use of 3D-printed valve models and experience is expected to be broadened in the near future, with the progress in material engineering, computer aided design and diagnostic imaging systems [9]. Although it seems a far stretch of imagination, in vivo implantation of 3D-printed aortic valves may become the finale goal [10].

2 Materials & Methods

The whole procedure of making the anthropomorphic silicone valve is illustrated in Figure 1, which contains following three main parts: suitable molding material selection, silicone perfusion and mold dissolving, final imaging validation using ultrasound and MRI.

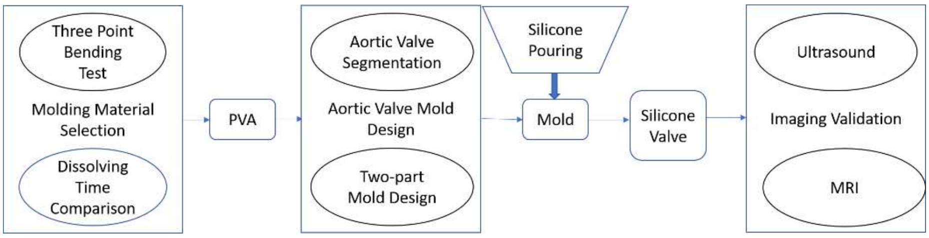

Fig. 1. Manufacturing procedure illustration & imaging compatibility validation

2.1 Molding Material Selection

Before using silicone to make the aortic valve phantom, a suitable molding material needs to be selected based on the following requirements: easy to dissolve with no additional solvents; stable when external force applied and slightly more flexible than general rigid printing materials like **Polylactic acid** (PLA). There are several water-soluble materials available on the printing market including **Polyvinyl alcohol** (PVA), High-T-Lay, Lay-PVA which fulfil these criteria [11]. In order to choose a suitable printing infill density and the best dissolving temperature, the chosen three molding materials were compared with different infills and at different water temperatures. The specimen for the infill density experiment was 3x3x3 $\boldsymbol{cm^3}$ cube with a discrete infill density range from 0% to 100%, while the specimen for the water temperature experiment was 1x1x1 $\boldsymbol{cm^3}$ cube with only 0% infill. The whole dissolving procedure was monitored by a surveillance camera (YI Dome Camera) and recorded from the starting point to fully dissolving point manually.

Meanwhile, a three-point bending test [12] was performed to compare the material flexibility and stability. The specimens for this test were 10x2x1 $\boldsymbol{cm^3}$ cuboids with infill density range from 20% to 100%. The machine used was a Zwick Roell Z010 tensile testing system and the experimental setup is shown in Figure 2. The recorded data were analyzed in Matlab 2019. The failure force when the sample cracks is simply the maximum loading force and the flexural modulus that represents the materials' flexibility needs to be calculated using equation 1 [12], where $\boldsymbol{E_f}$ is flexural modulus, L is support span, b is the width and d is the depth of the specimen and m is the gradient of the initial straight-line portion of the load-deflection curve:

$$\boldsymbol{E_f = (L^3 m)/(4bd^3)} \quad (1)$$

Fig. 2. Three-point bending test setup

2.2 Valve Manufacturing

After performing the above experiments, it was found that the most suitable molding material to make the internal mold is PVA, while the external mold can be printed with normal PLA for reuse. The original solid valve model was segmented from a healthy human chest CT scan using ITK-SNAP (University of Pennsylvania, USA) thresholding and region growing, then smoothed using a median filter in Seg3D (The University of Utah, USA). Finally the hollow model was generated using the erosion-dilation method in Seg3D, the thickness of the valve being 2 mm and the whole segmentation can be viewed in Figure 3.

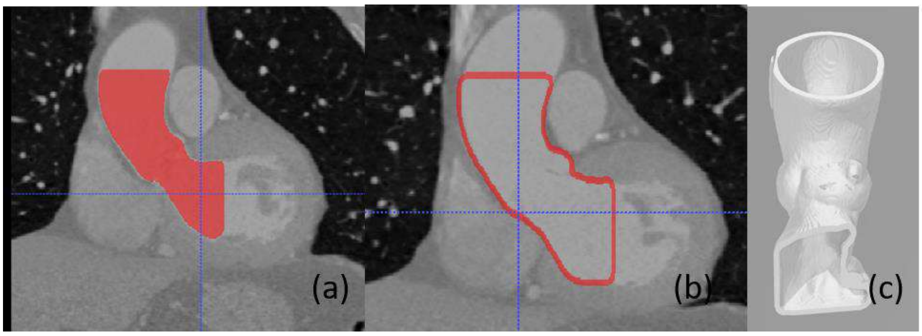

Fig. 3. Aortic valve model generation (a) Solid valve segmentation (b) Hollow valve segmentation and (c) 3D hollow valve model

After completing the valve segmentation, the 3D mold was designed using Solidworks 2018. The cavity was created based on the hollow model and the mold was then extracted as the external part (Figure 4(a)) and the internal part (Figure 4(b)). The external part was printed using rigid plastic PLA while the internal part was printed using PVA. With the assembled prints held with clamps (Figure 4(c)), the degassed ecoflex-silicone 0030 was poured into the mold and the basic normal valve model was manufactured as depicted in figure 4(d). Based on the normal silicone model, some pathological valve models were created as depicted in Figure 5, including a rheumatic one (Figure 5(b)), a calcified one (Figure 5(c)) and a bicuspid one (Figure 5(d)). Each valve model started with fused valve cusps..The rheumatic valve was created by ensuring the anatomical orifice consisted of cuts made one third down each valve closure line to recreate circumferential fusion of the cusps. The calcified valve was created by paint-brushing more silicone to replicate leaflet thickening and stiffening, while the bicuspid one was created by leaving one commissure fused to mimic a raphe.

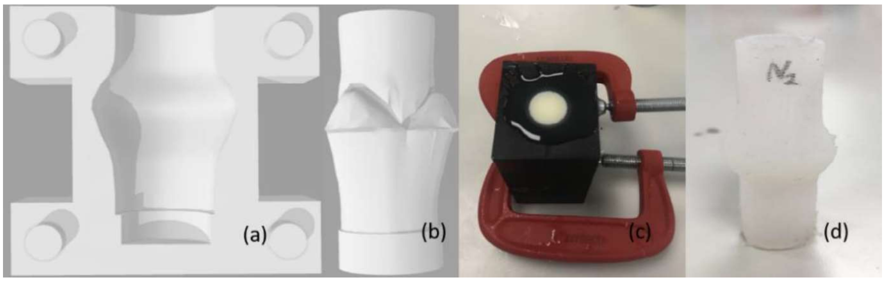

Fig. 4. Two-part mold-based silicone valve manufacturing (a) External mold (b) Internal mold (c) Two-part mold assembly and (d) Normal silicone valve

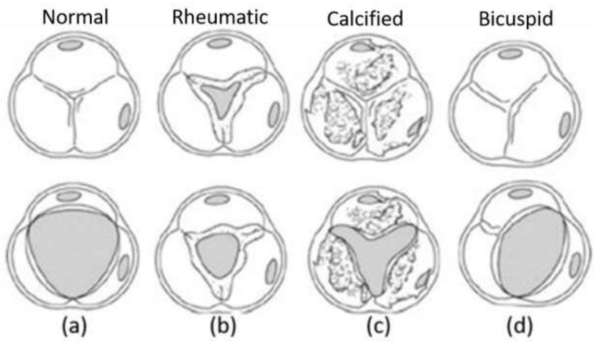

Fig. 5 [13]. Pathological valve models (a) Normal valve (b) Rheumatic valve (c) Calcified valve and (d) Bicuspid valve

2.3 US & MRI Imaging

To validate whether the valve phantoms can give the desired imaging results, the four types of silicone valves were imaged using 2D ultrasound and 3D MRI. The 2D ultrasound images were acquired on the Philips IE33 system with a S5-1 probe in water using the standard aortic valve short-axis view. For the 2D MR imaging, the silicone valves were connected to a commercial flexible silicone aorta phantom (T-S-N 005, Elastrat) and perfused by an MRI-compatible pulsatile flow pump (CardioFlow 5000 MR). This time the images were acquired in 1% Agar for optimized imaging results. Both imaging procedures are demonstrated in figure 6, with figure 6(a) showing the ultrasound imaging and figure 6(b) showing the MR imaging.

Fig. 6. Imaging validation (a) Ultrasound imaging and (b) MR Imaging

3 Results & Discussions

3.1 Molding Material Selection

Table 1. Molding material dissolving time comparison with different infill densities (@ room temperature 25 ℃).

Infill Density (%)	Time Taken to Dissolve (hours)		
	PVA	High-T-Lay	Lay-PVA
0	1.62	36.08	4.75
20	10.43	163.08	58.38
40	24.43	367.50	173.42
60	116.42	656.42	284.73
80	263.33	858.25	397.57
100	377.83	1028.17	494.28

Table 2. Molding material dissolving time comparison with different temperatures (@ 0% infill density).

Temperature (°C)	Time Taken to Dissolve (Minutes)		
	PVA	High-T-Lay	Lay-PVA
25	93	2124	311
40	72	1324	314
60	50	1293	309
80	42	1290	310
100	33	1285	306

Table 3. Molding material failure force comparison

Infill Density (%)	Maximum Load Force (N)		
	PVA	High-T-Lay	Lay-PVA
20	134	111	216
40	163	157	497
60	165	297	546
80	326	429	737
100	435	522	1152

The mold material dissolving comparisons are presented in Table 1 and Table 2. From Table 1, it is clear that PVA is the easiest to dissolve while High-T-Lay is the most difficult and the dissolving time increases non-linearly with the tested infill densities. Table 2 gives a similar result showing that PVA is the best water-soluble material at various water temperatures, while with higher temperature, all the tested materials will dissolve faster. Table 3 gives the failure force results of the materials, from which we can see Lay-PVA can withstand the highest external force and PVA can withstand the least, while with higher infill density, all the specimens' failure force increases. Regarding to the flexibility, PVA has the smallest flexural modulus and Lay-PVA has the largest, which means PVA is the best option with the requirement for flexible molding materials. With less infill density, the mold will be very fragile and the final printing option for the internal molding material was chosen to be PVA with 40% infill density.

Table 4. Molding material flexural modulus comparison

Infill Density (%)	Flexural Modulus (MPa)		
	PVA	High-T-Lay	Lay-PVA
20	137	489	612
40	144	705	906
60	148	972	1276
80	276	1244	1815
100	506	1656	2454

3.2 Valve Manufacturing

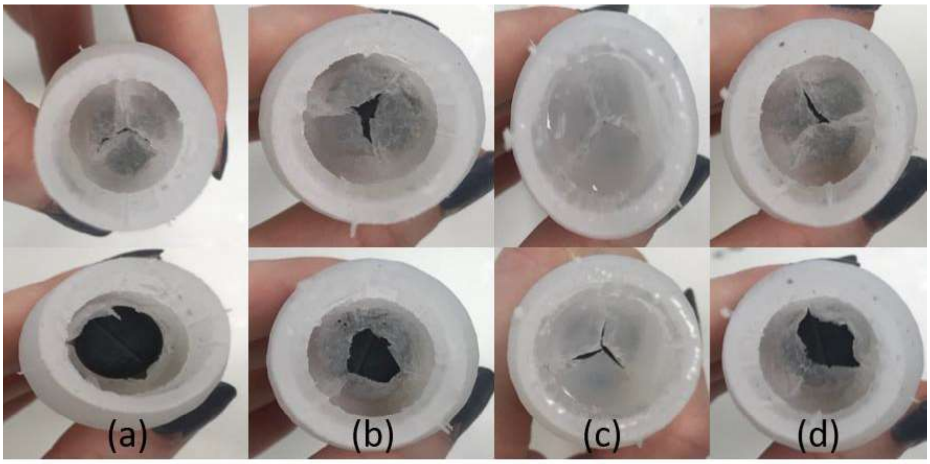

Fig. 7. Manufactured silicone valves, close on top, and open on the bottom (a) Normal valve (b) Rheumatic valve (c) Calcified valve and (d) Bicuspid valve

Figure 7 demonstrates the final fabricated valves using ecoflex-silicone 0030. From the results we can see the normal valve can open fully under pressure, while the rheumatic one can only open partially as the leaflets stick to each other, the calcified valve can barely open due to the abnormal thickness of the leaflets and the bicuspid one opens only on one side due to the incomplete leaflets. However, there is still the need for validating the valves' performance under different imaging modalities.

3.3 US &MRI Imaging

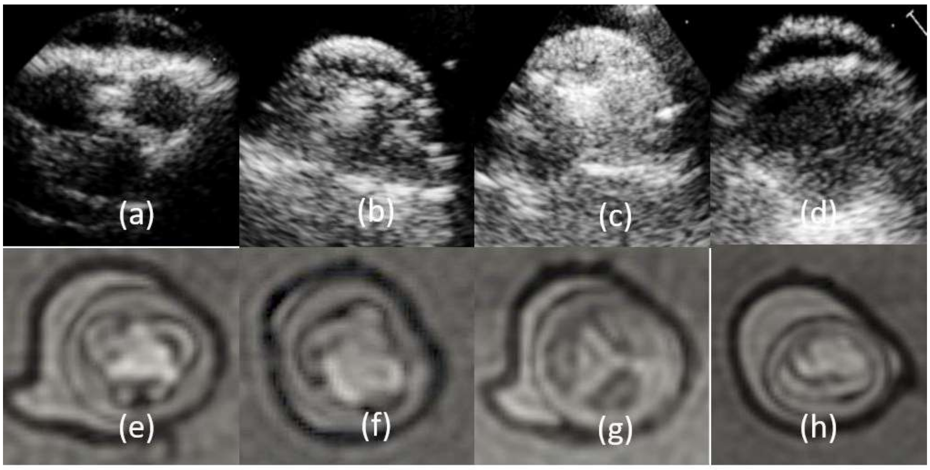

Fig.8. 2D Ultrasound images of (a) Normal valve (b) Rheumatic valve (c) Calcified valve and (d) Bicuspid valve; MR Images of (e) Normal valve (f) Rheumatic valve (g) Calcified valve and (h) Bicuspid valve

Figure 8 shows both the ultrasound and MR images of the four types of aortic valves from the short-axis view. Even though the ultrasound images are less clear and the difference is less significant, we can still see the normal valve has a perfect clear leaflet structure, while the rheumatic and calcified one have more vague anatomies and the bicuspid one demonstrates the abnormal opening from one side of the leaflets. The MR images show the full opening of the normal valve, however, under the same pressure, the rheumatic valve and calcified valves open much less, while the bicuspid one opens eccentrically.

These imaging results qualitatively demonstrate the imaging compatibility and functionality of the artificial valves made using 3D printing.

4 Conclusion & Future Work

In this paper, we propose a novel and easy method to fabricate soft aortic valve models, using PVA, the best water-soluble printing material, to make an internal mold and PLA to make the external mold. The molding material was chosen based on its dissolving performance and flexural modulus. The fabricated silicone valves are compliant, as the human heart valves and were shown to be ultrasound- and MRI- compatible. These valves may be useful in the future for studying valve function under normal and pathological conditions.

Future work will focus on quantitative evaluation of 3D-printed valve performance and development of direct silicone printing for manufacturing these valves, thus simplifying the process further.

References

1. Laura Ann Hockaday, Bin Duan, Kevin Heeyong Kang: 3D Printed Hydrogel Technologies for Tissue-Engineered Heart Valves, 3D Printing and Additive Manufacturing, vol 1(3): 122-136, Mary Ann Liberty INC (2014).
2. Gry Everborn, Henrik Schirmer: The Evolving Epidemiology of Valvular Aortic Stenosis. The Tromso Study, Heart 2013, vol 99: 396-400, (2013).
3. Fabrizio Donati, Saul Myerson: Beyond Bernoulli, Improving the Accuracy and Precision of Noninvasive Estimation of Peak Pressure Drops, Circulation: Cardiovascular Imaging, vol 10: 1-9, (2017)
4. Qian Z, Wang K, Liu S, et al: Quantitative Prediction of Paravalvular Leak in Transcatheter Aortic Valve Replacement Based on Tissue-Mimicking 3D Printing. JACC Cardiovasc Imaging. ;10(7):719-731, (2017)
5. Yancheng Wang, Bruce l. Tai, Hongwei Yu, et al: Silicone-Based Tissue-Mimicking Phantom for Needle Insertion Simulation, Transaction of the ASME, 8: 021001-1–021001-7, (2014)
6. Byrne N, Velasco Forte: A Systematic Review of Image Segmentation Methodology Used in the Additive Manufacture of Patient-specific 3D Printed Models of the Cardiovascular System. JRSM Cardiovasc Dis, vol 5, (2016)
7. Kan Wang: Controlling the Mechanical Behaviour of Dual-material 3D Printed Meta-materials for Patient-specific Tissue-mimicking Phantoms. Materials and Design, vol 90: 704-712, (2016)
8. Fabian Adams: Soft 3D-Printed Phantom of the Human Kidney with Collection System, Annals of Biomedical Engineering, vol 45 (4): 963-972, (2017)
9. Bompotis G: Transcatheter Aortic Valve Implantation Using 3D Printing Modelling Assistance. A Single-center Experience, Hellenic Journal of Cardiology, (2019)
10. Mohamad Alkhouli: 3D Printed Models for TAVR Planning, JACC: Cardiovascular Imaging, vol 10(7): 732-734, (2017)
11. https://all3dp.com/kai-parthy-shares-3d-printing-soluble-filaments-lay-away/
12. Zweben, C., W. S. Smith, and M. W. Wardle: Test Methods for Fibre Tensile Strength, Composite Flexural Modulus, And Properties of Fabric-Reinforced Laminates, Composite Materials: Testing and Design (Fifth Conference), ASTM International, (1979)
13. Baumgartner Huang: Recommendations on the Echocardiographic Assessment of Aortic Valve Stenosis: A Focused Update from the European Association of Cardiovascular Imaging and the American Society of Echocardiography, Eur Heart J Cardiovasc Imaging, vol 18(3): 254-275, (2017)